

# Petrographical and geochemical signatures of Jurassic rocks of Chari Formation, Western India: implications for provenance and tectonic setting

Shaista Khan<sup>1</sup> · A. H. M. Ahmad<sup>1</sup> · M. Masroor Alam<sup>2</sup> · Adnan Quasim<sup>1</sup>

Received: 27 January 2015 / Revised: 2 December 2015 / Accepted: 29 December 2015 / Published online: 16 January 2016  
© Science Press, Institute of Geochemistry, CAS and Springer-Verlag Berlin Heidelberg 2016

**Abstract** The sandstones of the Ridge and Athleta members of Chari Formation (Callovian-Oxfordian) exposed at Jara have been analyzed for their petrographical and geochemical studies. Texturally, these sandstones are medium to coarse grained, poorly to well sorted, sub-angular to sub-rounded, and show low to medium sphericity. These sandstones were derived from a mixed provenance including granites, granite-gneisses, low and high-grade metamorphic, and some basic rocks of Aravalli range and Nagarparkar massif. The petrofacies analysis reveals that these sandstones belong to the continental block and recycled orogen tectonic regime. The studied sandstones are modified by paleoclimate, distance of transport, and diagenesis. Mineralogically and geochemically, sandstones are classified as quartzarenite, subarkose, arkose, sublithic arenite, and wacke, respectively. The A-CN-K ternary plot and CIA, CIW, PIA, and ICV values suggest that the similar source rocks suffered moderate to high chemical weathering under a hot-humid climate in an acidic environment with higher  $P_{CO_2}$ . Generally good to strong correlations between  $Al_2O_3$  and other oxides in these sediments indicate clay mineral control. The  $K_2O/Na_2O$  versus  $SiO_2$  diagram indicates that the studied samples occupy passive margin fields but the  $SiO_2/Al_2O_3$  versus  $K_2O/Na_2O$  plot suggests that the Athleta Sandstone and

Ridge Sandstone fall within the passive margin field, while Ridge Shale falls within the active continental margin field.

**Keywords** Petrography · Geochemistry · Jurassic rocks · Chari Formation · Kachchh · Gujarat

## 1 Introduction

Kachchh is a peri-continental, paleo-rift basin on the westernmost fringe of the Indian peninsula (Biswas 1987). The basin occupies the entire district of Kachchh in the Gujarat State of western India, close to its western border with Pakistan, between latitude  $22^{\circ}30' - 24^{\circ}30'N$  and longitude  $68^{\circ} - 72^{\circ}E$  (Fig. 1). The basin is situated at the southern edge of the Indus shelf perpendicular to the southern Indus fossil rift (Zaigham and Mallick 2000). It is bounded by the Nagar Parker fault in the north, Radhanpur–Barmer arch in the east and Kathiawar fault towards the south (Biswas 1982). The Mesozoic sediments are exposed in the form of six discontinuous domal areas: (a) Kachchh Mainland, (b) Pachham Island, (c) Khadir Island, (d) Bela Island, (e) Chorar Island, and (f) Wagad. Mesozoic sediments ranging in age from Bajocian to Albian (Rajnath 1932; Singh et al. 1982; Fürsich et al. 2001) (Table 1) lay unconformably on the Precambrian basement (Bardan and Datta 1987). The Kachchh Basin is a collage of three lithopackages viz. Mesozoic, Tertiary and Quaternary. The Mesozoic package comprises of Late Triassic to Early Jurassic continental, Middle to Late Jurassic marine, and Late Jurassic to Early Cretaceous fluvio-deltaic sediments. Mesozoic sediments are rift fill sediments and constitute the major part of the basin fill. The Tertiary sediments, on the other hand, are mostly shallow marine shelf sediments in the peripheral and

✉ Shaista Khan  
shaista.khans03@gmail.com

<sup>1</sup> Department of Geology, Aligarh Muslim University, Aligarh, UP, India

<sup>2</sup> Geology Section, Civil Engineering, Z.H. College of Engineering and Technology, Aligarh Muslim University, Aligarh, UP, India

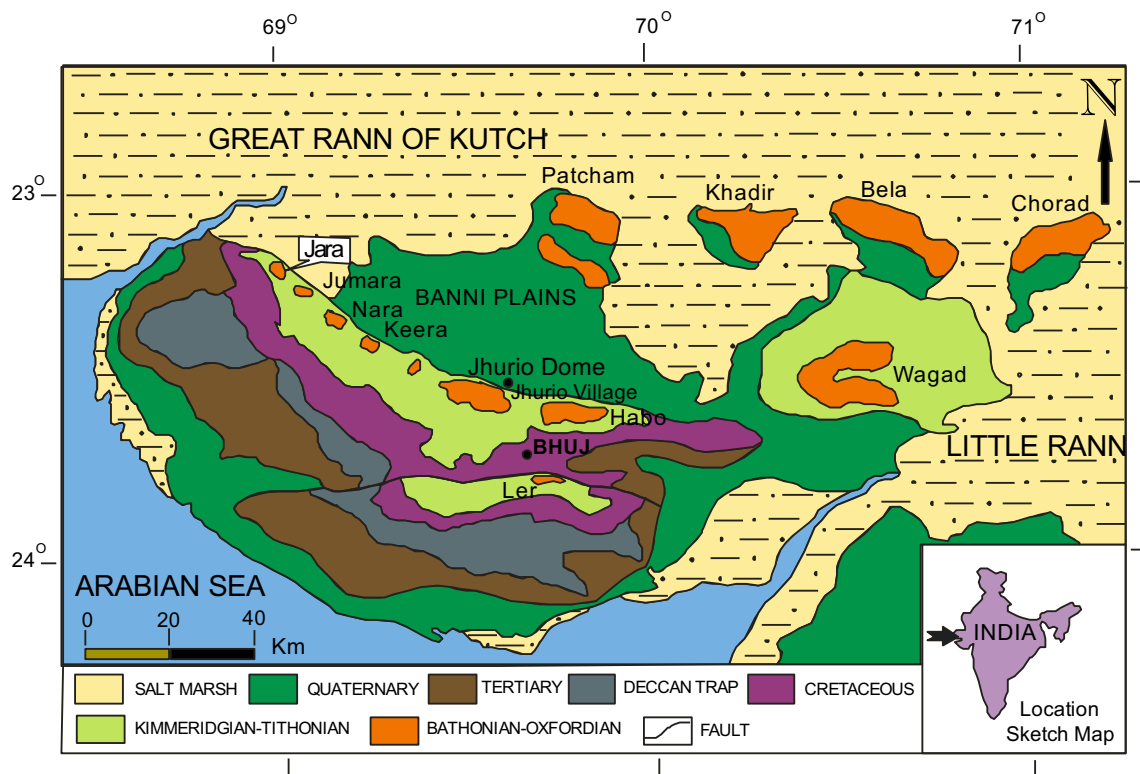


**Fig. 1** Geological map of Kachchh Basin (after Biswas 1977)

**Table 1** Lithostratigraphic framework of the Jurassic and Lower Cretaceous rocks of Kachchh Mainland (Fürsich et al. 2001)

Age	Kachchh mainland	
Albian-Aptian	Umia Formation	Bhuj Member Ukra Member
Neocomian		Ghuner Member
Tithonian		Umia Member
Tithonian-Kimmeridgian	Katrol Formation	
Late Early Oxfordian		Dhosa Oolite Member
Early Oxfordian	Chari Formation	Dhosa Sandstone Member Gypsiferous Shale Member Athleta Sandstone Member
Callovian		Ridge Sandstone Member Shelly Shale/Keera Golden Oolite Member
Bathonian	Patcham Formation	Sponge Limestone Member Purple Sst./Echinodermal Packstone Member Jumara Coralline Limestone Member
Bajocian-Bathonian	Jhurio Formation	Goradongar Yellow Flagstone Member Jhura Golden Oolite Member Canyon Lst./Badi Golden Oolite Member Badi White Limestone Member

intervening structural lows bordering the Mesozoic uplift areas. The study area, the Jara Dome, is situated on the northwestern fringe of the northern flexure zone (NFZ) of the Kachchh mainland. It is a quaquaversal dome, 3 km in

diameter, bounded by the North latitudes of 23°43'–23°45' and the East longitudes of 68°57'–69°00'.

The most important aspect of the lithostratigraphy of the Jara Dome is represented by the Chari Formation

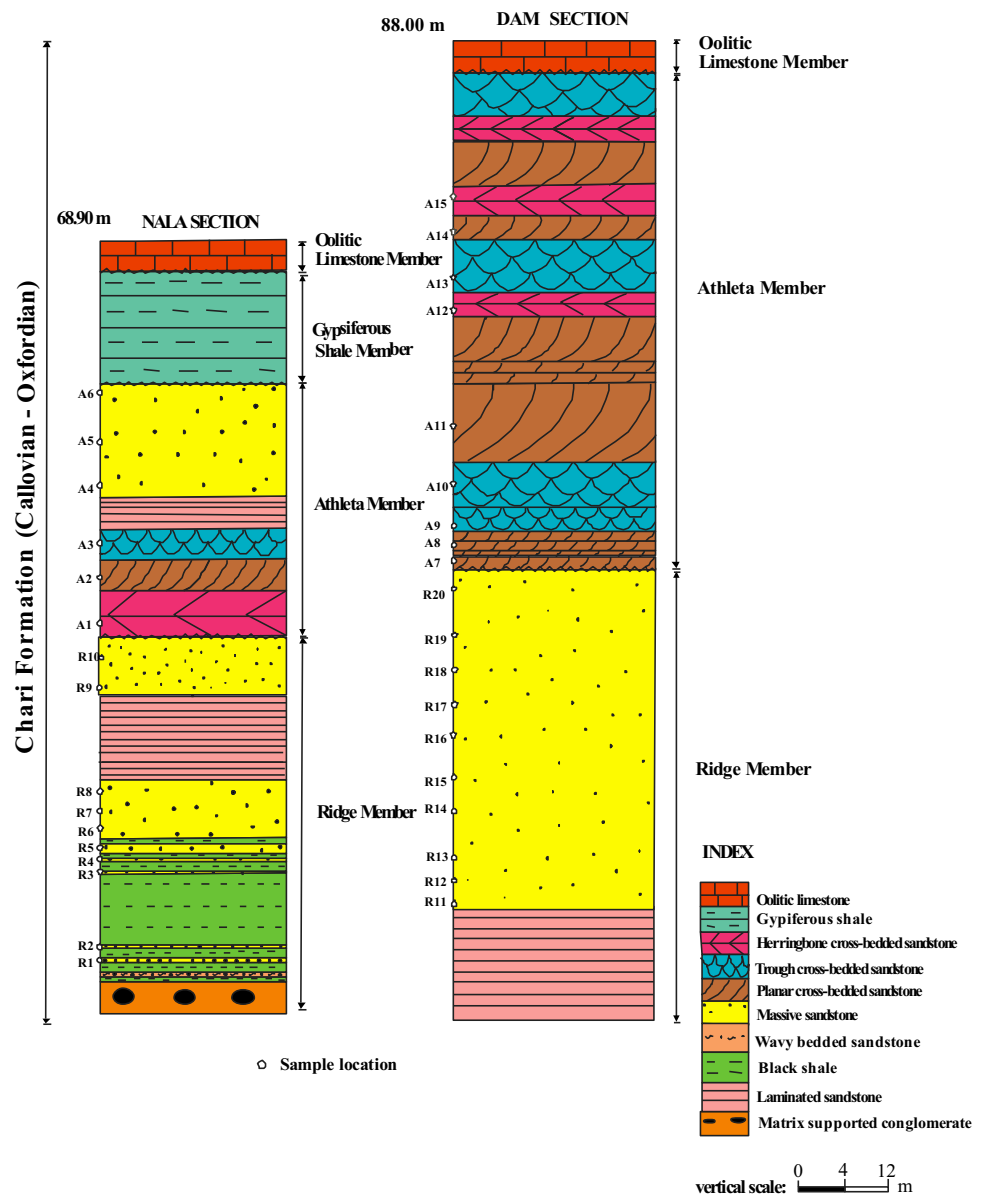
(Callovian-Oxfordian) which is mainly exposed into two sections. These two measured sections are 68.90 and 88.00 m thick, and are mainly composed of matrix supported conglomerate, shale, sandstones, gypsiferous shale, and oolitic limestone (Fig. 2). The present study provides the first detailed reports on the petrography and geochemistry of sandstone and shales from the Chari Formation (Jara Dome) in order to evaluate the provenance, tectonic setting, paleoweathering, and paleoclimatic conditions during their deposition. The petrofacies analysis reveals that these sandstones belong to the continental block, recycled orogen, and rifted continental margin tectonic regime. The present petrofacies is the result of mixing of detritus from the granite-gneiss basement uplift, on the one hand, and from the metasedimentary rocks of a

recycled orogen, on the other. The paleocurrent direction for planar cross-bedded sandstone of Chari Formation is SSW followed by WSW and, for trough cross-bedded sandstone, is WNW followed by NNW.

### 2 Geological setting

The majority of the Indian peninsula is a shield area with intracratonic and pericratonic fault bounded basins. More than half the area of exposed peninsula is constituted of Archean gneisses, schists, and Precambrian meta-sediments and meta-igneous rocks. The rest of the peninsula is covered by volcanic flows (Deccan and Rajmahal trap), Late Precambrian–Early Paleozoic sediments, and

**Fig. 2** Measured lithostratigraphic sections from Jara Dome, Kachchh, Gujarat



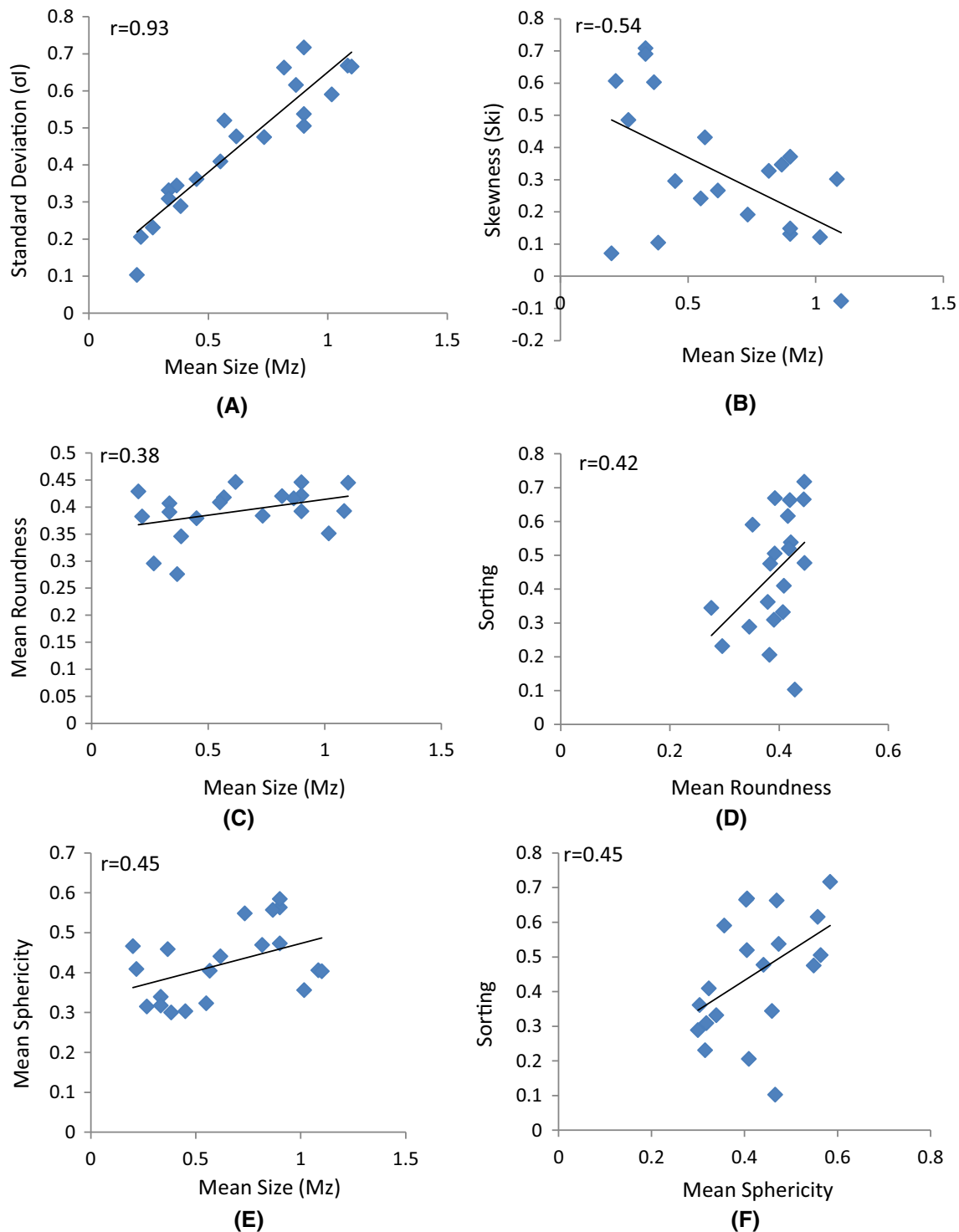
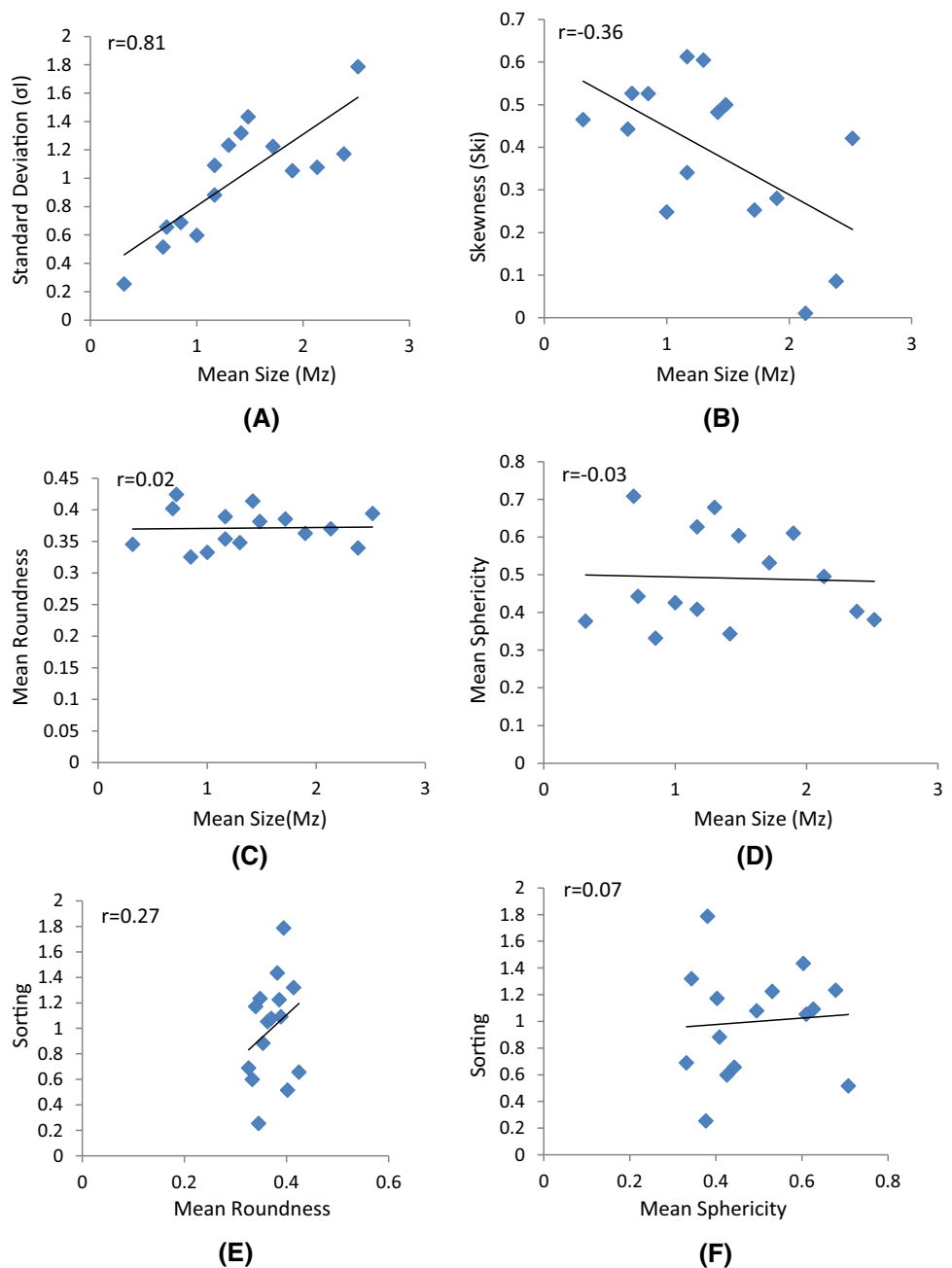


**Fig. 3** Bivariant plot of **a** Mean size versus standard deviation, **b** Mean size versus Skewness, **c** Mean size versus mean roundness, **d** Mean roundness versus sorting, **e** Mean size versus mean sphericity, **f** Mean sphericity versus sorting of Ridge Sandstone Member, Kachhh Basin

Gondwana rocks. According to Cannon et al. (1981) and Tankard et al. (1982), the beginning of plate separation in the Gondwanaland during Jurassic and Early Cretaceous was marked by the formation of pericratonic rift basins.

The pericratonic rifts (e.g. Kachhh and Saurashtra) represent parts of an elongated extensional trough where vertical rifting during Jurassic–Cretaceous time brought about basin formation and sedimentation. This proactive/

**Fig. 4** Bivariant plot of **a** Mean size versus standard deviation, **b** Mean size versus skewness, **c** Mean size versus mean roundness, **d** Mean roundness versus sorting, **e** Mean size versus mean sphericity, **f** Mean sphericity versus sorting of Athleta Sandstone Member, Kachchh Basin



retroactive rifting event produced sediment repositories (Jurassic of Kachchh) later in the southern part (Early Cretaceous of Saurashtra) (Casshyap and Aslam 1992).

Much of the Mesozoic sedimentation took place during the early rift phase of the evolution of India's western continental margin. At first, the basin margin of the Nagar Parkar Fault and the Island Belt Fault (Kaladongar–Khadir–Bela fault system) was filled up by granite-cobble fanglomerates and arkoses. Then the sag region between the Island belt and Mainland was filled by continental to paralic valley fill clastics dated as Rhaetic by Koshal (1984). The first marine transgression started with the

extension of graben up to the Kathiawar upliftment by the activation of the north Kathiawar fault during the rift–rift transition of the Indian plate movement. The graben was inundated forming a gulf. The carbonates of the basin were deposited during this period. In Early Oxfordian time, the proto-oceanic stage was reached with complete inundation of the embayed basin. The rifting failed by the Early Cretaceous time when the clastics of the prograding delta filled up the basin as the sea regressed (Biswas 1982). The first occurrence of marine sediments in the middle Jurassic (Bajocian) indicates that this graben became a fully marine basin during that time.

**Table 2** Percentages of detrital minerals in the sandstones of Jara Dome, Kachchh, Gujarat

S. No.	Monocrystalline Quartz	Polycrystalline quartz		Feldspar		Mica		Chert	Rock fragments	Heavies
	Common Quartz	Recrystallized metamorphic Quartz	Stretched metamorphic Quartz	Plagioclase	microcline	Muscovite	Biotite			
Athleta Sandstone Member										
A1	84.02	0.33	1.20	0.00	8.65	2.00	0.00	1.00	1.01	0.56
A2	82.44	1.00	0.77	0.56	10.00	4.11	0.01	1.09	0.11	0.65
A3	72.11	3.50	3.00	1.23	11.56	3.23	0.00	1.34	1.45	0.90
A4	73.05	4.00	0.89	2.00	14.50	5.00	0.00	1.00	0.11	0.11
A5	86.33	1.25	1.45	1.00	5.11	1.22	0.40	0.23	2.00	0.00
A6	87.23	3.50	0.55	1.56	4.97	2.00	0.00	0.54	0.56	0.00
A7	81.34	2.10	0.12	1.50	9.56	1.45	0.11	1.45	1.11	0.10
A8	75.65	5.00	2.00	1.11	10.00	2.46	0.00	0.33	0.00	0.00
A9	76.45	4.23	1.22	1.78	11.24	2.10	0.10	0.00	1.54	0.00
A10	85.35	2.56	0.30	0.56	4.87	3.09	0.00	0.65	0.00	0.57
A11	85.45	1.45	1.45	0.00	7.49	1.07	0.23	0.00	0.45	0.00
A12	81.66	4.22	1.66	1.22	6.20	1.55	0.00	0.76	0.89	0.32
A13	84.50	3.87	0.54	0.32	8.00	1.43	0.00	0.00	1.08	0.12
A14	83.45	3.02	0.78	0.21	8.89	2.00	0.70	0.87	0.00	0.00
A15	79.45	6.70	2.10	0.11	6.56	1.01	0.00	1.23	0.86	0.67
Avg.	81.23	3.12	1.20	0.88	8.51	2.25	0.10	0.70	0.74	0.27
Ridge Sandstone Member										
R1	88.67	3.09	0.06	0.00	3.45	1.78	0.01	0.81	0.62	0.67
R2	80.00	2.00	1.13	1.45	9.68	1.67	0.00	1.04	0.00	0.00
R3	72.23	2.56	4.87	1.01	11.00	4.45	0.03	2.00	0.04	0.87
R4	75.98	3.98	0.64	0.00	13.23	4.32	0.00	0.37	1.09	0.32
R5	85.56	2.06	1.45	0.65	5.34	2.67	1.45	0.56	0.00	0.00
R6	83.66	1.34	1.32	0.82	7.03	2.00	0.00	1.24	0.86	0.00
R7	85.00	0.06	0.04	0.05	9.00	5.01	0.00	0.00	0.00	0.09
R8	74.03	2.43	3.00	1.22	11.04	4.09	0.00	1.03	1.54	0.90
R9	75.35	3.21	0.11	1.13	14.65	3.98	0.00	1.88	0.00	0.00
R10	86.16	2.14	1.56	0.45	4.85	2.00	0.00	0.06	2.00	0.02
R11	86.50	1.30	1.61	0.50	4.77	2.23	0.00	0.00	2.10	0.78
R12	78.09	4.39	0.00	1.14	10.45	1.54	0.01	0.45	1.50	0.69
R13	85.45	3.06	0.05	0.56	7.47	1.12	0.00	0.00	1.67	0.01
R14	83.11	4.56	0.00	0.00	5.56	3.56	0.34	0.00	0.50	0.00
R15	81.00	6.98	2.30	0.02	5.67	1.04	0.00	0.87	0.78	0.56
R16	76.17	6.55	1.12	1.67	10.63	2.87	0.78	0.00	0.23	0.00
R17	80.00	3.02	1.73	1.89	7.34	1.66	0.00	0.77	2.00	0.54
R18	86.56	4.12	1.78	0.00	3.09	1.59	0.00	0.01	1.98	0.00
R19	79.09	5.03	1.34	1.32	8.67	1.04	0.00	0.00	1.00	0.67
R20	84.66	6.00	0.00	0.72	5.09	1.09	0.82	0.87	0.00	0.22
Avg.	81.36	3.39	1.21	0.73	7.90	2.49	0.17	0.60	0.90	0.32

### 3 Methodology

The study is based on the field analysis of the stratigraphic sections and the petrographic examination of representative sandstone samples (Fig. 2). Sixty-five samples of medium

to coarse grained sandstone of the Ridge and Athleta members were collected from Jara Dome. Textural and mineralogical studies are based on thirty-five representative samples. Terminology of Krynine (1948) and Folk (1980) is followed when describing varieties of quartz and

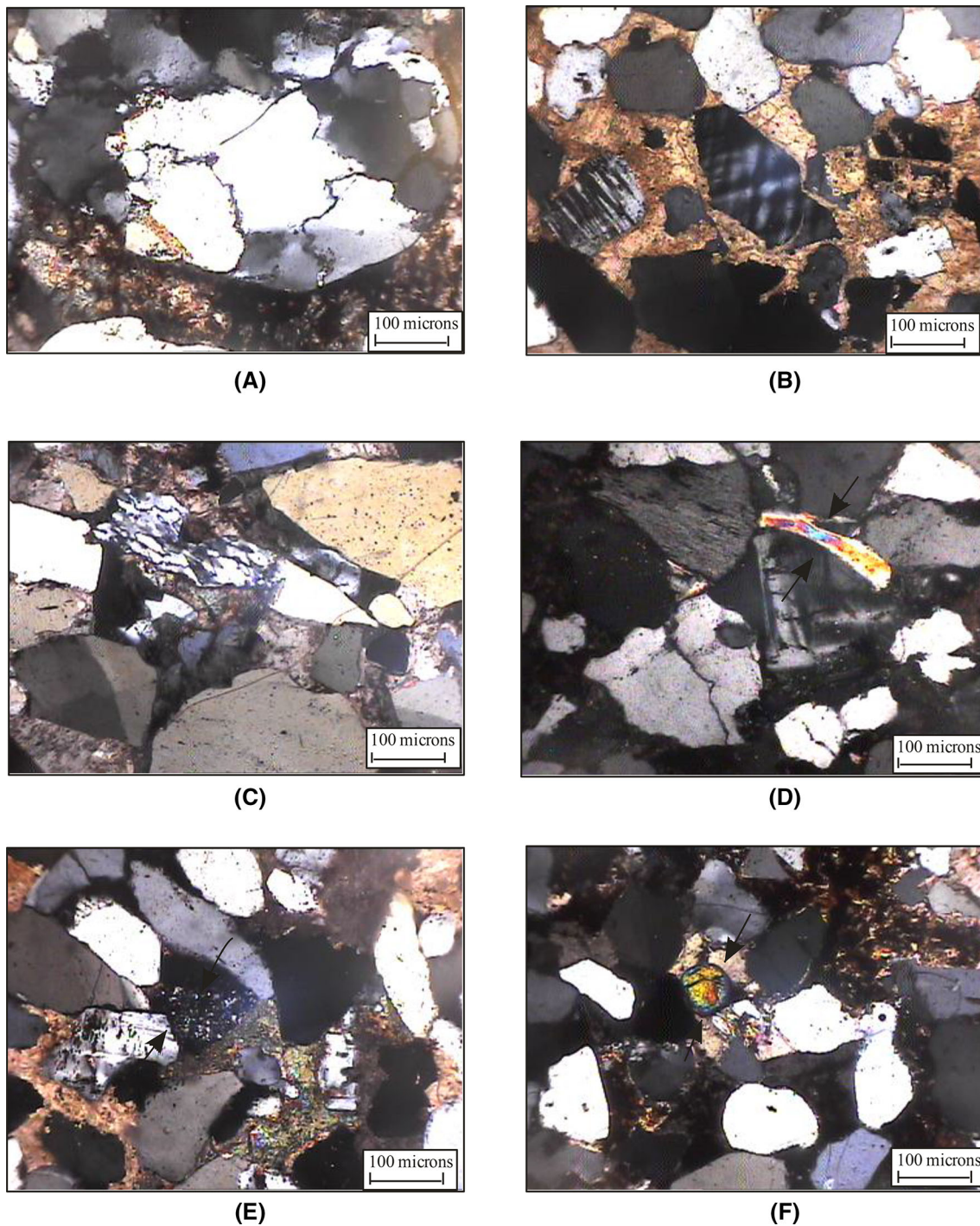
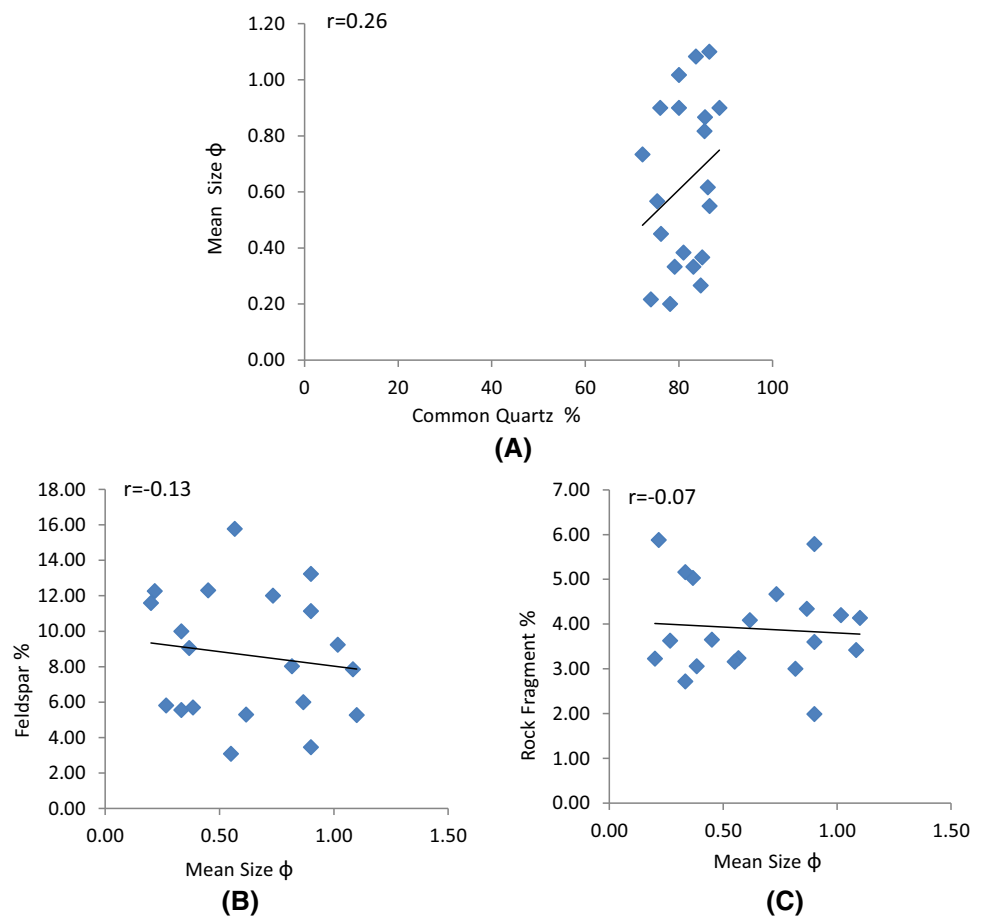


**Plate I** Photomicrographs showing **a** quartz grain, **b** fresh feldspar grain, **c** weathered feldspar grain, **d** muscovite grain, **e** chert grain, **f** zircon

other framework constituents. Grain size measurements were carried out with the help of a micrometer eyepiece. Two hundred and fifty framework grains were counted per thin section. The grid spacing used in the point counting exceeded the grain size, so as to avoid individual grains being counted more than once (Van Der Plas and Tobi

1965). After useful thin section screening, altogether 30 representative samples (21 sandstone and 9 shale) were selected for geochemical analysis. For major element analysis, the X-ray fluorescence spectrometer at N.I.O. Goa, AXIOS model of PAN Analytical, Netherlands was used.

**Fig. 5** Bivariant plots of mean size versus common quartz (a), feldspar (b), and rock fragments (c) of Ridge Sandstone. (N = total number of samples, r = correlation coefficient)



#### 4 Ridge Sandstone Member

The graphic mean size values of the Ridge Sandstone Member ranged from  $0.20\phi$  to  $1.10\phi$ , with an average of  $0.63\phi$  (coarse to medium grained). Sorting values ranged from  $0.10\phi$  to  $0.72\phi$ , with an average of  $0.45\phi$  (moderately well sorted to well sorted). Skewness values ranged from  $-0.08$  to  $0.71$ , with an average of  $0.32$  (Strongly fine skewed followed by fine skewed). Kurtosis values ranged from  $0.78$  to  $1.91$ , with an average of  $1.19$  (leptokurtic followed by mesokurtic). Grains are sub-angular to sub-rounded. The mean roundness of individual samples ranged from  $0.28$  to  $0.45$ , with an average of  $0.39$ . The mean sphericity values of studied samples range from  $0.30$  to  $0.48$ , with an average of  $0.42$ .

##### 4.1 Bivariants plots of textural parameters

The mean size values of Ridge Sandstones, plotted against their sorting values and their correlation coefficient values, is computed as  $0.93$  (high relationship) (Fig. 3a). The mean size versus skewness plots gives a correlation coefficient value of  $-0.54$  (moderate relationship) (Fig. 3b). The mean size versus roundness plot gives a correlation

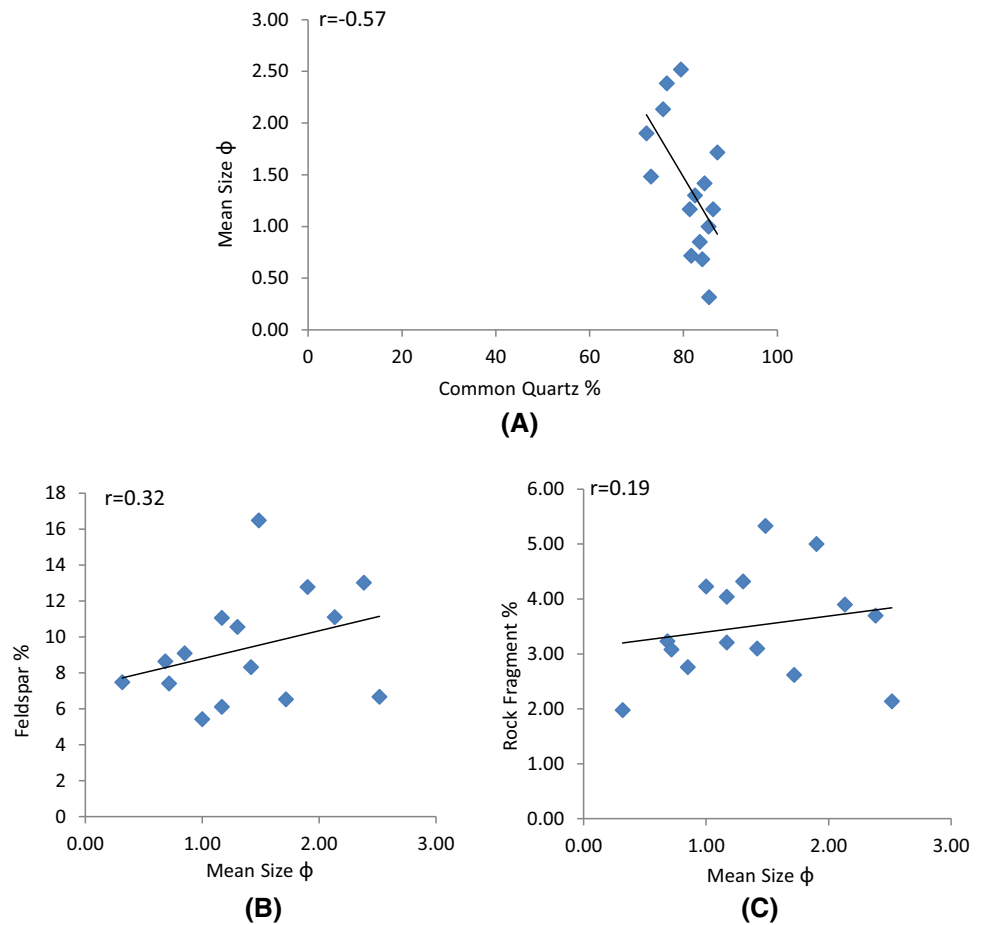
coefficient value of  $0.38$  (moderate relationship) (Fig. 3c). The mean size versus sphericity diagram has a correlation coefficient of  $0.42$  (moderate relationship) (Fig. 3d). The plot of roundness versus sorting gives a correlation coefficient value of  $0.45$  (moderate relationship) (Fig. 3e). The plot of sphericity versus sorting has a correlation coefficient value of  $0.45$  (moderate relationship) (Fig. 3f).

##### 4.2 Interpretation

The textural study of the twenty samples of the Ridge Sandstone Member shows that they are coarse to medium grained, moderately well sorted to well sorted, strongly fine skewed to fine skewed, and leptokurtic to mesokurtic. The samples are generally sub-angular to sub-rounded and show low to moderate sphericity. Bivariant plots of different parameters indicate that the mean size versus sorting has high relationship, indicating increase in grain size with increased sorting, which reflects constant hydrodynamic condition during deposition. Mean size versus skewness has a moderate relationship and the samples are strongly fine skewed to fine skewed in a normal range of mean size, indicating fluctuation in the energy condition of the depositional medium. Mean size versus sphericity has a



**Fig. 6** Bivariant plots of mean size versus common quartz (a), feldspar (b), and rock fragments (c) of Athleta Sandstone. (N = total number of samples, r = correlation coefficient)



moderate relationship, indicating a decrease in sphericity with increase in grain size. Roundness versus sorting has a moderate relationship, giving indication of increased in roundness with sorting. Sphericity versus sorting has moderate relationship also suggests increase in sphericity with sorting (Khan 2010; Ahmad et al. 2015).

## 5 Athleta Sandstone Member

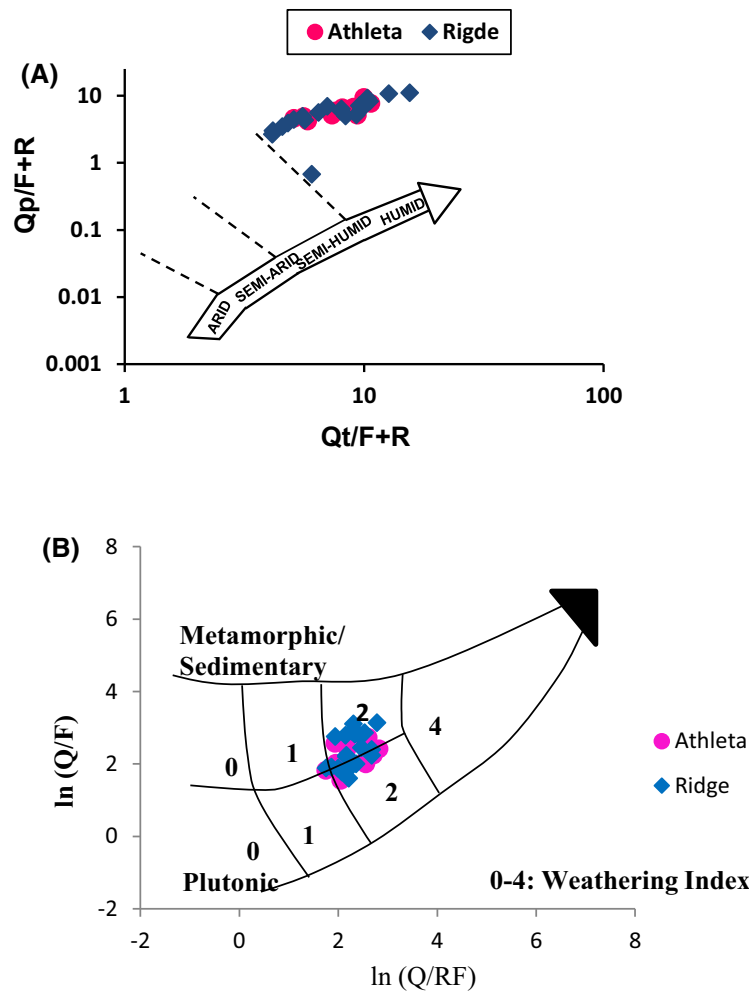
The graphic mean size value of Athleta Sandstones ranged from  $0.32\phi$  to  $2.52\phi$ , with an average of  $1.38\phi$  (medium to coarse grained). Sorting values ranged from  $0.25\phi$  to  $1.79\phi$ , with an average of 1.00 (poorly to moderately well sorted). Skewness values ranged from 0.01 to 0.61, with an average of 0.39 (strongly fine skewed followed by fine skewed). Kurtosis values ranged from 0.86 to 1.89, with an average of 1.16 (most of the samples are leptokurtic followed by mesokurtic). Grains are sub-angular to sub-rounded. The mean roundness of individual samples ranged from 0.33 to 0.41, with an average of 0.37. The mean sphericity value ranged from 0.33 to 0.71, with an average of 0.49.

### 5.1 Bivariant plots of textural parameters

The mean size values of the Athleta Sandstones are plotted against their sorting values; their correlation coefficient value is 0.81 (high relationship) (Fig. 4a). The mean size versus skewness plot gives a correlation coefficient value of  $-0.36$  (moderate relationship) (Fig. 4b). The mean size versus roundness plot gives a correlation coefficient value of 0.02 (poor relationship) (Fig. 4c). The mean size versus sphericity diagram has a correlation coefficient of 0.03 (poor relationship) (Fig. 4d). The plot of the roundness versus sorting gives a correlation coefficient value of 0.27 (poorly sorted) (Fig. 4e). The plot of sphericity versus sorting has a correlation coefficient value of 0.07 (poorly sorted) (Fig. 4f).

### 5.2 Interpretation

The textural study of fifteen sandstone samples of Athleta Member shows that they are medium to coarse grained, poorly to moderately well sorted, strongly fine skewed to fine skewed, and leptokurtic to mesokurtic. The sand grains are sub-angular to sub-rounded and show medium to low



Semi-quantitative Weathering index		Physiography (relief)		
		High (Mountain)	Moderate (Hill)	Low (Plains)
		0	1	2
Climate (Precipitation)	(Semi) Arid and Mediterranean	0	0	0
	Temperate subhumid	0	1	2
	Tropical humid	0	2	4

**Fig. 7** **a** Bivariant log/log plot for Jara Dome sandstones, Kachchh Basin, according to Suttner and Dutta (1986). **b** Log ratio plot after Weltje et al. (1998). *Q* quartz, *F* feldspar, *RF* rock fragments

sphericity. Large populations of sub-angular to sub-rounded grains indicate a short transportation of sediments. However these features may remain so even after long distances of transport (Pettijohn 1975). Bivariant plots of various parameters indicate that the mean size versus sorting has a good relationship, indicating an increase in grain with increased sorting, which reflects constant hydrodynamic condition during deposition. Mean size

versus skewness has a moderate relationship and the samples are strongly fine skewed to fine skewed, in a narrow range of mean sizes, indicating fluctuation in the energy condition of the depositional medium. Mean size versus mean roundness has a poor relationship, indicating a decrease in roundness with decreasing grain size. Mean size versus sphericity has a poor relationship, giving a hint of a decrease in sphericity with increase in grain size.

**Table 3** Major element abundance of Athleta Sandstone, Ridge Sandstone and Ridge Shale of Jara Dome, Kachchh, Gujarat

	SiO <sub>2</sub>	Al <sub>2</sub> O <sub>3</sub>	TiO <sub>2</sub>	Fe <sub>2</sub> O <sub>3</sub>	MnO	MgO	CaO	Na <sub>2</sub> O	K <sub>2</sub> O	P <sub>2</sub> O <sub>5</sub>	CIA	CIW	PIA	ICV
Athleta Sandstone														
Avg.	87.79	2.88	0.47	3.10	0.02	1.07	0.07	0.07	0.60	0.06	82.72	94.35	93.32	0.93
Max.	97.86	5.52	2.49	5.95	0.09	4.42	0.55	0.55	1.57	0.21	94.16	98.04	97.45	2.20
Min.	73.82	1.44	0.06	0.54	0.01	0.01	0.01	0.01	0.02	0.02	61.99	74.39	67.98	0.36
Ridge Sandstone														
Avg.	72.38	11.09	0.51	4.64	0.08	1.01	0.56	0.56	2.46	0.11	69.20	84.03	79.34	0.96
Max.	76.02	16.05	0.91	9.71	0.12	1.75	0.72	0.72	2.98	0.18	75.50	88.72	86.33	1.18
Min.	66.98	6.02	0.09	0.94	0.04	0.24	0.39	0.39	1.91	0.07	61.78	78.46	70.49	0.84
Ridge Shale														
Avg.	62.87	22.86	1.27	7.15	0.02	1.49	0.48	0.58	2.70	0.14	82.33	92.16	91.07	0.66
Max.	69.95	26.25	1.46	11.69	0.08	2.24	0.74	0.76	2.89	0.19	86.02	95.54	94.98	0.86
Min.	56.67	14.38	0.93	5.50	0.00	1.01	0.27	0.41	2.24	0.10	77.09	88.67	86.67	0.52

Oxides in wt%

**Table 4** Correlation coefficient among chemical parameters of Athleta Sandstone, Ridge Sandstone and Ridge Shale, Jara Dome, Kachchh, Gujarat

	Athleta Sandstone	Ridge Sandstone	Ridge Shale
Al <sub>2</sub> O <sub>3</sub> – SiO <sub>2</sub>	–0.95	–0.97	–0.75
Al <sub>2</sub> O <sub>3</sub> – TiO <sub>2</sub>	0.60	0.98	0.96
Al <sub>2</sub> O <sub>3</sub> – MgO	0.73	0.77	0.52
Al <sub>2</sub> O <sub>3</sub> – Na <sub>2</sub> O	0.70	0.79	–0.02
Al <sub>2</sub> O <sub>3</sub> – K <sub>2</sub> O	0.96	0.99	0.83

Roundness versus sorting has a moderate relationship, giving an indication of increase in roundness with sorting. Sphericity versus sorting has a poor relationship, giving hint of an increase in sphericity.

## 6 Detrital mineral composition

The detrital content comprises quartz, feldspar, mica, chert, rock fragments, and heavy minerals. The latter occurs as a minor constituent. The average composition of the detrital minerals of sandstones are: Quartz, 85.79 %, Feldspar, 8.95 %; Mica, 2.53 %; Chert, 0.64 %; Rock fragments, 0.83 % (phyllite, schist, siltstone and claystone); Heavy minerals, 0.26 % (opaques, zircon, tourmaline, biotite, rutile, garnet, epidote and staurolite). The Ridge Sandstone is represented by 85.96 % quartz; 8.63 % feldspar; 2.66 % mica; 0.60 % chert; 0.90 % rock fragments, and 0.32 % heavy minerals. The Athleta Sandstone consists of 85.55 % quartz, 9.38 % feldspar, 2.35 % mica, 0.70 % chert, 0.74 % rock fragments, and 0.27 % heavy minerals (Table 2) (Plate-Ia–f).

## 7 Relationship of size to framework detrital minerals

Distribution of a mineral and/or minerals in sandstones is not controlled or affected by size of the constituent grains. This is especially true of feldspar and rock fragments, as the former are generally known to increase in grain size and the latter decrease in grain size. The relationship between mean size, on one hand, and various types of detrital constituents i.e., quartz, feldspar and rock fragments, on the other hand, were studied with help of a bivariate diagram and correlation coefficient (Figs. 5, 6).

The relationship of size to sandstone composition was studied by plotting mean size versus percentages of quartz, feldspar and rock fragments. There is no significant correlation between mean size and composition except the Athleta Sandstone, in which a moderate relationship exists between mean size and quartz.

## 8 Factors controlling detrital mineralogy

Paleoclimate, distance of transport, source rock composition and diagenesis are the most important factors controlling composition at the time of deposition. These factors were studied in detail in order to analyze their effect on detrital composition.

Bivariate log/log plot of the ratio of polycrystalline quartz to feldspar plus rock fragments (Suttner and Dutta 1986) has been used for interpreting the paleoclimate of the Ridge and Athleta Sandstones. The mean values of the ratio indicate a humid climate for the area (Fig. 7a). The paleoclimate simulations for the Jurassic and Lower Cretaceous times show India as a part of the Gondwanaland

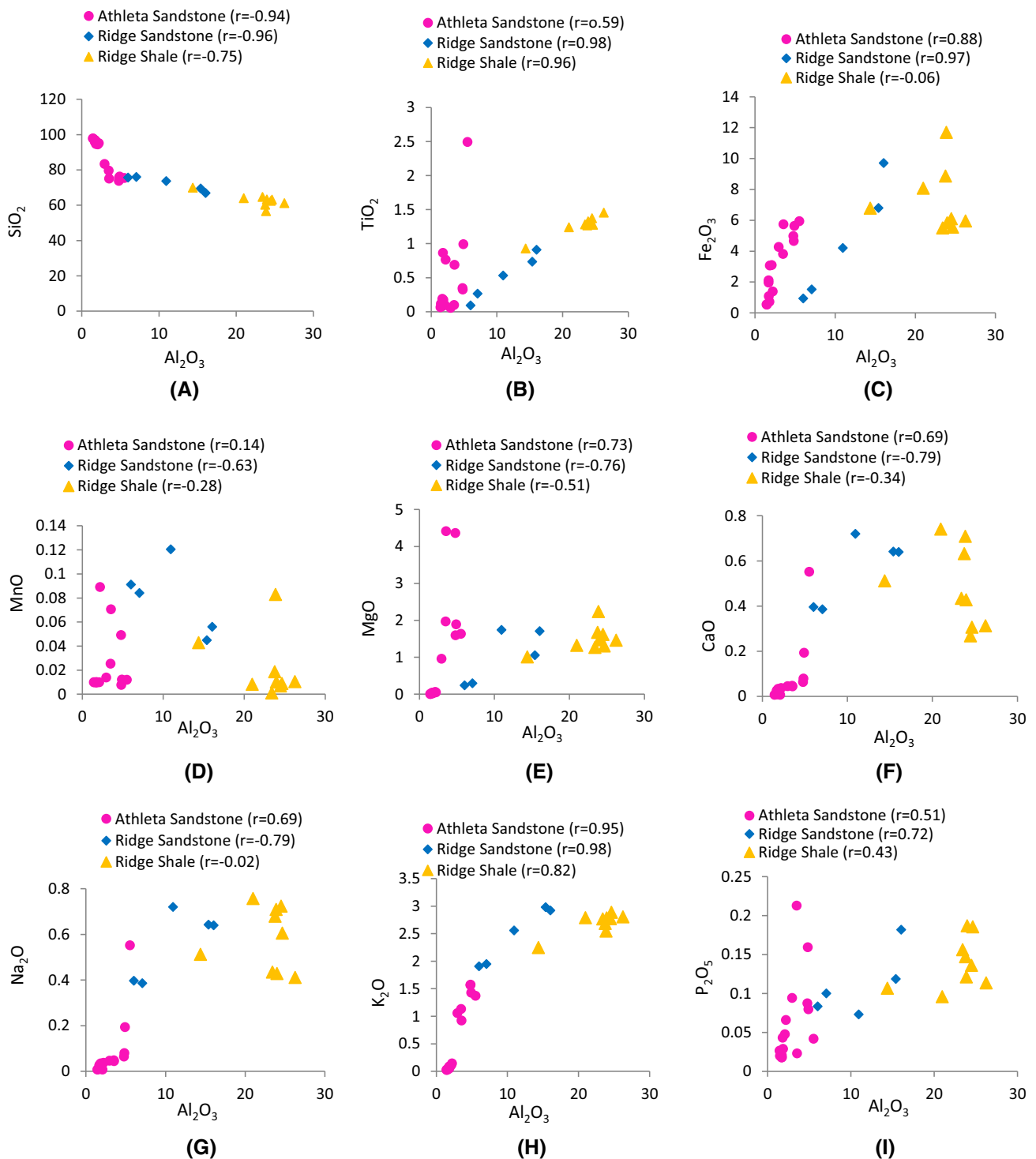


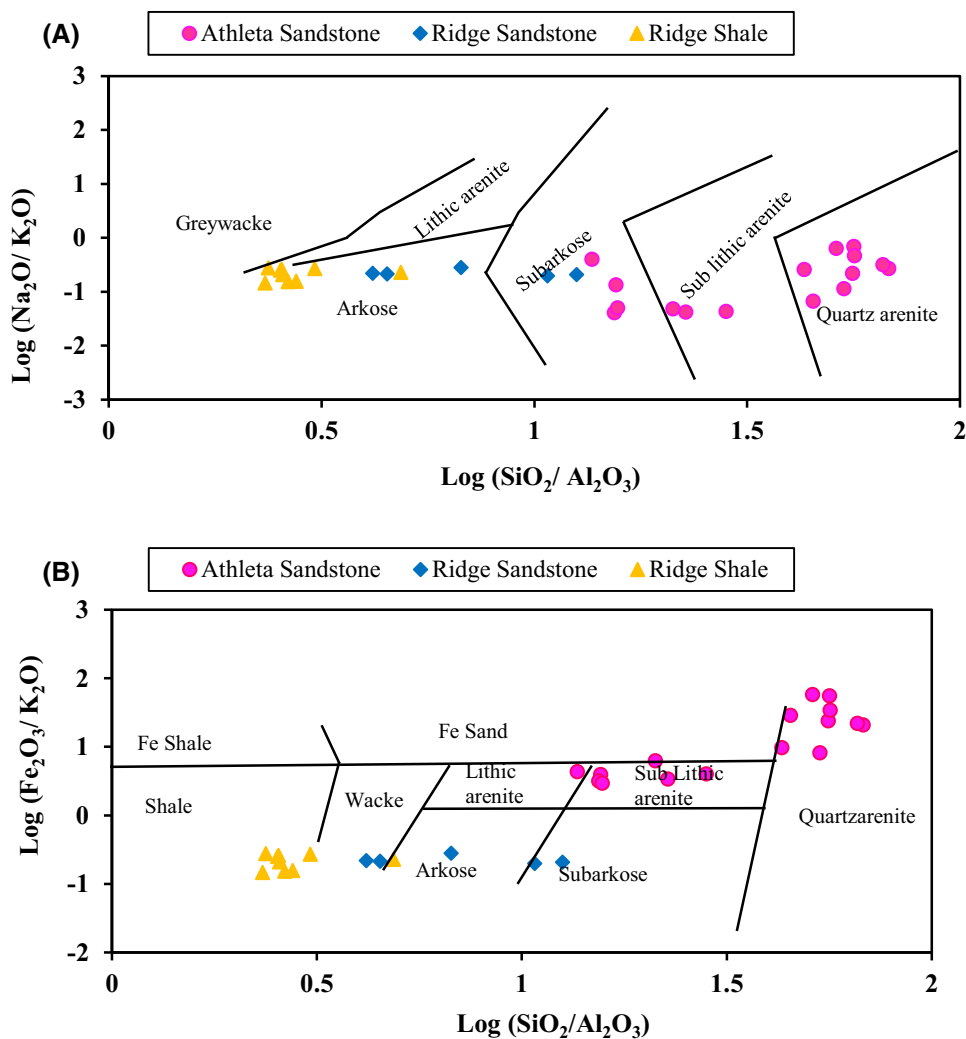
**Fig. 8**  $Al_2O_3$  versus major oxides covariation diagram

that experienced humid to tropical climate (Thompson and Barron 1981; Chatterjee and Hotton 1986; Chandler et al. 1992).

The precipitation of huge carbonate during the Jurassic is also supportive of the fact that the area was witnessing a warm climate similar to that found in tropics. A

combination of low relief, hot humid climate and ample vegetation can produce quartz rich detritus (Franzinelli and Potter 1983). Low relief provides prolonged the residence time of sediments, thereby increasing the detritus of chemical weathering and thus the sediments in the stable quartz. Overall study suggests that such a strong

**Fig. 9** **a**  $\text{Log} (\text{Na}_2\text{O}/\text{K}_2\text{O})$  versus  $\text{Log} (\text{SiO}_2/\text{Al}_2\text{O}_3)$  plot (Pettijohn et al. 1987) for geochemical classification of the Jara Dome sediments. **b**  $\text{log} (\text{Fe}_2\text{O}_3/\text{K}_2\text{O})$  versus  $\text{log} (\text{SiO}_2/\text{Al}_2\text{O}_3)$  plot (Herron 1988) for geochemical classification of the Jara Dome sediments



chemical weathering condition is an unconformity within worldwide humid and warm climate during the Jurassic period (Thompson and Barron 1981). The mineralogical data plotted on the Weltje et al. (1998) diagram falls in the field number 2, which points to the sedimentation in a low relief and tropical humid conditions (Fig. 7b). Therefore, the Aravalli range and Nagarparkar massif rocks, which provided sediments to the Kachchh rift, must have undergone rigorous weathering under humid tropical conditions, resulting in the destruction of much of the feldspar and labile constituents. Thus, climate might have been an important factor in the production of compositional mature quartz rich sandstones. However, climate alone cannot produce quartz rich sands.

The suite of heavy minerals present in the studied sandstones, including zircon and rutile, may have been derived from silicic igneous and crystalline metamorphic rocks (Friedman and Johnson 1982). The brown variety of tourmaline is derived from pegmatized injected metamorphic terrains, the green from granitic rocks, and the blue

from pegmatites (Krynine 1946). However, well-rounded tourmaline has been derived from a sedimentary source, indicating more than one cycle of transport. On the other hand, the suite of heavy minerals, including garnet and staurolite, points to a metamorphic source. However, the occurrence of various shades of garnet indicates different source rocks, from acid igneous to metamorphic rocks. Muscovite was derived from low-grade metamorphic rocks (Folk 1980). Epidote may have been derived from crystalline metamorphic rocks. The presence of tourmaline, garnet, and zircon suggests that the energy of the depositional agency was higher. These heavy mineral suites in the Ridge and Athleta Sandstones reflect their source in the mixed assemblage of acid and basic igneous rocks and low to high grade metamorphic rocks, such as those believed to represent the eroded and weathered parts of the present day Aravalli range situated east and northeast of the basin and Nagarparkar massif situated to the north and northwest (Dubey and Chatterjee 1997). The detrital grains of the Ridge and Athleta Sandstones are in sand size range and

derived from the Aravalli Range, suggesting transportation over a distance of a few hundred kilometers. The studied sandstones are a small amount of feldspar and one possible reason for this deficiency may be the transportation of sediments by high gradient streams and the rapid destruction of feldspar by abrasion. Since deposition of the Ridge and Athleta Sandstones took place in a tectonically active

rift, the presence of high gradient stream is quite likely within the basin. However this premise does not stand to scrutiny, because rock fragments that could have been destroyed more easily are common within studied sandstones. Therefore some factor other than transportation was responsible for the paucity of feldspar in both of the studied sandstones. Feldspar was removed to a large extent in the humid climatic condition by chemical weathering. The replacements of quartz by carbonate and iron oxide cement in the studied sandstones suggest the modification of the composition of the sandstones. The presence of weathered feldspars grains, as well as oversize pores, indicate the dissolution of detrital grains in the studied sandstones. The study of grain contacts of the sandstones indicates that the sandstones were subjected to compaction during burial, and that their original texture and fabric were slightly modified by the processes of compaction.

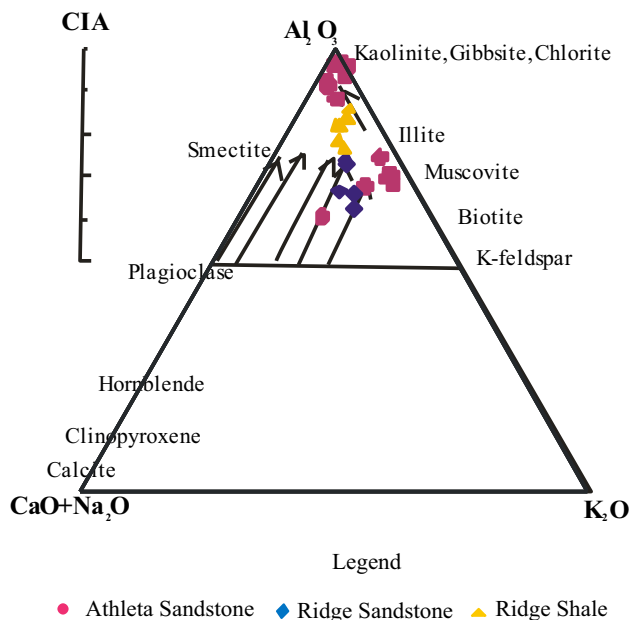
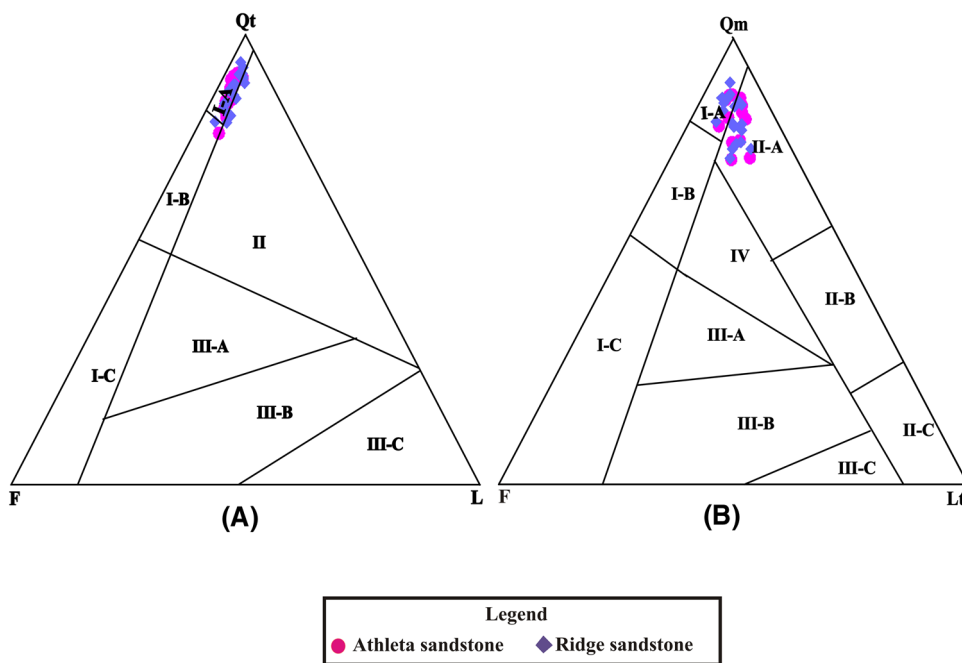


**Fig. 10** A-CN-K (in molecular proportion) ternary plot (Nesbitt and Young 1982) for the Jara Dome sediments. *Ka* Kaolinite, *Gi* Gibbsite, *Ch* Chlorite, *Pl* Plagioclase, *Ksp* K-feldspar

### 9 Major element geochemistry

Major element data indicate that the sandstones of the Athleta Member largely composed of SiO<sub>2</sub> varying from 73.82 % to 97.86 % (average 87.79 %). In these sandstones the Al<sub>2</sub>O<sub>3</sub> concentration varies from 1.44 % to 5.52 % (average 2.88 %), Fe<sub>2</sub>O<sub>3</sub> from 0.54 % to 5.95 % (average 3.10 %), MgO from 0.01 % to 4.42 % (average 1.07 %), K<sub>2</sub>O from 0.02 % to 1.57 % (average 0.60 %), and Na<sub>2</sub>O from 0.01 % to 0.55 %, (average 0.07 %), respectively. For TiO<sub>2</sub>, the contents show large variations:

**Fig. 11** Classification of the sandstones of Jara Dome, Kachchh (according to Dickinson 1985). The provenance field in A and B are continental Block (I): I-A: Craton Interior, I-B: Transitional Continent, I-C: Continent uplift, Recycled Orogen (II): II-A Quartzose, II-B: Transitional, II-C: Lithic Magmatic Arc (III): III-A: Dissected, III-B: Transitional III-C: Undissected and Mixed (IV). *Qt* total quartz, *Qm* monocrystalline quartz, *F* feldspar, *L* total unstable lithic fragments, *Lt* total lithic fragments



0.06 % to 2.49 % (average 0.47 %). The CaO content show small variation between 0.01 and 0.55 % (average 0.07 %), except three samples which possessed anomalously high values of 0.19 % and 0.55 % (Table 3).

The SiO<sub>2</sub> concentration within the Ridge Sandstone samples varied from 66.98 % to 76.02 % (average 72.38 %) (Table 3). In these sandstones, Al<sub>2</sub>O<sub>3</sub> varies from 6.02 % to 16.05 % (average 11.09 %) and Fe<sub>2</sub>O<sub>3</sub> from 0.94 to 9.71 % (average 4.64 %). The TiO<sub>2</sub> and MgO contents show small variation compared to the Athleta Sandstone, which is 0.09 % to 0.91 % (average 0.51 %) and 0.24 % to 1.75 % (average 1.01 %), respectively. Similarly, the range of variation in CaO, K<sub>2</sub>O, and Na<sub>2</sub>O content is also small i.e. 0.39 % to 0.72 % (average 0.56 %), 1.91 % to 2.98 % (average 2.46 %), and 0.39 % to 0.72 % (average 0.56 %), respectively.

The SiO<sub>2</sub> concentration within the Ridge Shale samples ranged from 56.67 % to 69.95 % (average 62.87 %) (Table 3). The Al<sub>2</sub>O<sub>3</sub> content varied from 14.38 % to

26.25 % (average 22.86 %). The TiO<sub>2</sub> content showed narrow variation from 0.93 % to 1.46 % (average 1.27 %) and so did the K<sub>2</sub>O and Na<sub>2</sub>O values, 2.24 % to 2.89 % (average 2.70 %) and 0.41 % to 0.76 % (average 0.58 %), respectively, while the Fe<sub>2</sub>O<sub>3</sub> concentration varied from 5.50 % to 11.69 % (average 7.15 %). The MgO and CaO values ranged from 1.01 % to 2.24 % (average 1.49 %) and 0.27 % to 0.74 % (average 0.48 %), respectively.

The correlation matrix indicates a certain association in the sandstones and shale of Jara Dome (Table 4). In the Athleta Sandstone, Ridge Sandstone and Ridge Shale samples, Al<sub>2</sub>O<sub>3</sub> shows a strong negative relationship with SiO<sub>2</sub> ( $r = -0.95; -0.97; -0.75$ ); a moderate to strong positive relationship with TiO<sub>2</sub> ( $r = 0.60; 0.98; 0.96$ ), K<sub>2</sub>O ( $r = 0.96; 0.99; 0.83$ ), P<sub>2</sub>O<sub>5</sub> ( $r = 0.52; 0.72; 0.44$ ). The Fe<sub>2</sub>O<sub>3</sub> content shows a strong positive relationship only in sandstones ( $r = 0.88; 0.97$ ) (Fig. 8). There is a strong positive correlation of MgO with Al<sub>2</sub>O<sub>3</sub> in the Athleta Sandstone ( $r = 0.73$ ) but equally negative correlation in Ridge Sandstone and Shale samples ( $r = -0.76; -0.51$ ), respectively. The generally good to strong correlation between Al<sub>2</sub>O<sub>3</sub> and oxides in these sediments indicate clay mineral control.

In the geochemical classification diagram of Pettijohn et al. 1987 the studied samples occupy the arkose, subarkose, sublitharenite, and quartzarenite fields (Fig. 9a). Herron (1988), modified the diagram of Pettijohn et al. (1987), using  $\log(\text{Fe}_2\text{O}_3/\text{K}_2\text{O})$  along the Y-axis instead of  $\log(\text{Na}_2\text{O}/\text{K}_2\text{O})$ . The ratio of Fe<sub>2</sub>O<sub>3</sub>/K<sub>2</sub>O allows the arkoses to be more successfully classified and is also a measure of mineral stability. A further advantage of the Herron classification is that it can be simultaneously used to distinguish shales, sandstones, arkose, and carbonate rocks. The studied samples occupy shale, wacke, arkose, subarkose, lithic arenite, sublitharenite, and quartzarenite fields in the Herron diagram (Fig. 9b).

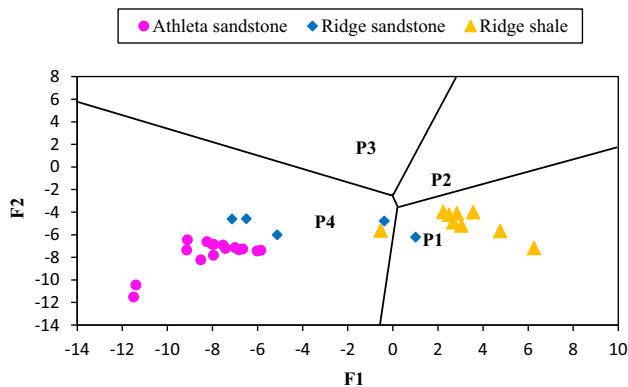


**Fig. 12** Discrimination function diagram (Roser and Korsch 1988) for Jara Dome sediments.  $F1 = (-1.773 \text{ TiO}_2 + 0.607 \text{ Al}_2\text{O}_3 + 0.76 (\text{Fe}_2\text{O}_3)^{\dagger} - 1.5 \text{ MgO} + 0.616 \text{ CaO} + 0.509 \text{ Na}_2\text{O} - 1.224 \text{ K}_2\text{O} - 9.09)$  and  $F2 = (0.445 \text{ TiO}_2 + 0.07 \text{ Al}_2\text{O}_3 - 0.25 (\text{Fe}_2\text{O}_3)^{\dagger} - 1.142 \text{ MgO} + 0.438 \text{ CaO} + 1.475 \text{ Na}_2\text{O} + 1.426 \text{ K}_2\text{O} - 6.861)$

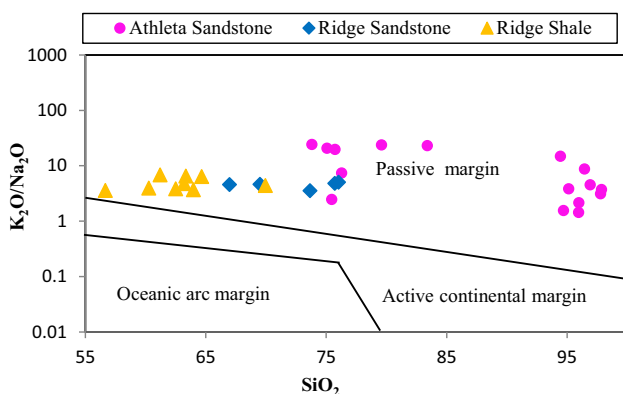


**Fig. 13** Tectonic setting discrimination for Jara Dome sediments after Roser and Korsch (1986). **a** Ocean Island Arc, **b** continental Island arc, **c** active continental margin, **d** passive margin

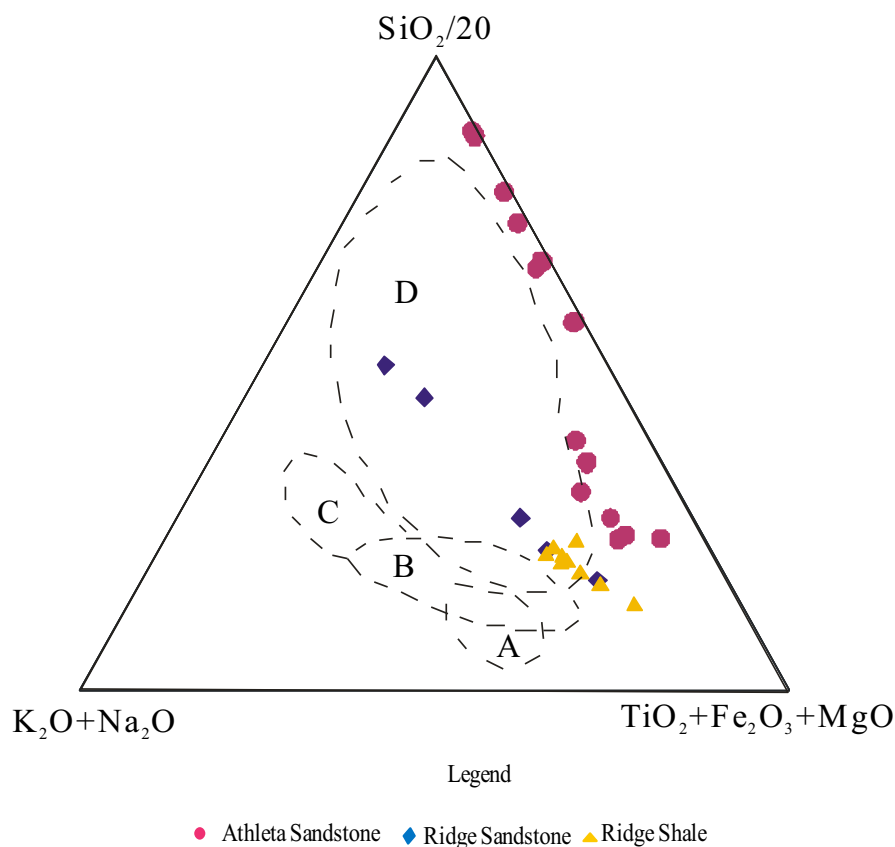
## 9.1 Paleoweathering conditions

The most widely used chemical index to ascertain the degree of source area weathering are the chemical index of alteration (CIA), chemical index of weathering (CIW) and plagioclase index of alteration (PIA). The CIA proposed by Nesbitt and Young (1982) was based on the calculation in terms of molecular proportion:

$$\text{CIA} = [\text{Al}_2\text{O}_3 / (\text{Al}_2\text{O}_3 + \text{CaO} * + \text{Na}_2\text{O} + \text{K}_2\text{O})] \times 100$$

The CIA values of the Athleta Sandstone ranged from 61.99 % to 94.16 %, with an average of 82.72 %, the Ridge Sandstone ranged from 61.75 % to 75.50 % (average 69.20 %), and the Ridge Shale values ranged from 77.09 % to 86.02 % (average 82.33 %). The CIA values of the sandstones and shale of the present study indicate that

**Fig. 14** Plot of the major elements composition of the Jara Dome sediments on the tectonic setting discrimination diagram



A. Ocean Island Arc, B. Continental Island arc, C Active continental margin, D. Passive margin

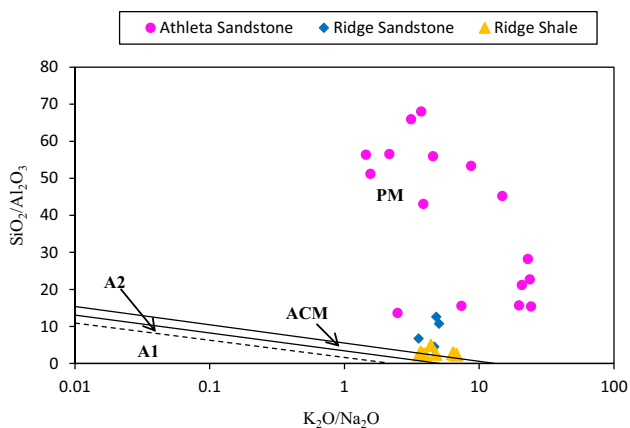


**Fig. 15** Tectonic setting discrimination diagram based on SiO<sub>2</sub>/Al<sub>2</sub>O<sub>3</sub> versus K<sub>2</sub>O/Na<sub>2</sub>O (after Maynard et al. 1982) for the Jara Dome sediments

the sediments have been derived from the source rocks that were subjected to both physical and chemical breakdown.

Chemical index of weathering (CIW)-For a better estimation of weathering conditions in source area many authors have used several indices (Fedó et al. 1995).

$$CIW = [Al_2O_3 / Al_2O_3 + CaO * + Na_2O] \times 100$$

The CIW values of the Athleta Sandstone, Ridge Sandstone and Ridge Shale ranged from 74.39 to 98.04 (average 94.35); 78.46 to 88.72 (average 84.03), and 88.67 to 95.54 (average 92.16), respectively. On the basis of the CIW, the studied sediments may be interpreted to show moderate to high chemical weathering.

Plagioclase index of alteration (PIA)—the chemical weathering can also be indicated by the PIA i.e. PIA (Fedó et al. 1995), especially when the plagioclase weathering needs to be monitored. The values are calculated using the following formula:

$$PIA = [(Al_2O_3 - K_2O) / (Al_2O_3 + CaO * + Na_2O - K_2O)] \times 100$$

The PIA values of the Athleta Sandstone, Ridge Sandstone and Ridge Shale range from 67.98 to 97.45 (average 93.32); 70.49 to 86.33 (average 79.34), and 86.67 to 94.98, (average 91.07), respectively. The PIA value of the studied sediments further ascribed moderate to intense plagioclase weathering in the source area.



Another method to measure the maturity of the rocks and assess the original composition of the sandstone and shale and their relation to the tectonic setting is quantified by calculating the the index of compositional variability introduced by Cox et al. (1995).

$$\text{ICV} = \frac{[\text{Fe}_2\text{O}_3 + \text{K}_2\text{O} + \text{Na}_2\text{O} + \text{CaO} * + \text{MgO} + \text{MnO} + \text{TiO}_2]}{\text{Al}_2\text{O}_3}$$

The ICV values of the Athleta Sandstone, Ridge Sandstone and Ridge Shale varies from 0.36 to 2.20 (average 0.93); 0.84 to 1.18 (average 0.96); 0.52 to 0.86 (average 0.66). These sediments are the product of recycled sediment deposited in the tectonically quiescent or cratonic environment.

The scattering shown by the A-CN-K plot data points probably represents a variable degree of weathering in the source terrain (Fig. 10). This may be the result of the non-steady state weathering conditions where active tectonism and uplift allow erosion of all soil horizons and rock surfaces (Nesbitt et al. 1997).

## 9.2 Provenance and tectonic setting

The plots of Jara Dome sandstones on the Qt-F-L and Qm-F-Lt (Fig. 11) diagram suggest that the detritus of the sandstones were derived from the granite-gneisses exhumed in the craton interior and low to high grade metamorphic supracrustal forming recycled orogen shedding quartzose debris of the continental affinity into the basin. It has been mentioned that the provenance of Jara Dome Sandstone is believed to be weathered parts of the present day Aravalli Range situated northeast, east and southeast of the basin and the Nagarparkar massif situated north and northwest of the basin. This is indicated by sand dispersal pattern studied by various workers (Balagopal and Srivastava 1975; Dubey and Chatterjee 1997; Ahmad et al. 2008). The two source areas are represented by the Precambrian metasediments and the granite-gneiss of Aravalli Supergroup. The present petrofacies evolve through the mixing of detritus from granite to gneiss basement uplift, on the one hand, and from metasedimentary rocks of a recycled orogen, on the other. The sediment composition was extensively modified during weathering under the warm, humid climate at the source area and by weathering during transport and sedimentation. Thus quartz rich detritus were shed into the Kachchh rift. The relief of the provenance was low and the erosion processes were not strong enough to remove the cover rocks from the basement.

The formation of mature quartzose sands, such as those of the Ridge and Athleta sandstones, have been ascribed to multicyclic reworking on cratons by several workers. However recent work has shown conclusively that the

quartzose sand is also being produced as a first-cycle sediment from the deeply weathered granite and gneissic bed rock exposed in the tropical low lands of the modern Amazon basin (Franzinelli and Potter 1983). The lack of second cycle grain of quartz suggests that recycling was perhaps not an important factor in the formation of quartz rich Ridge and Athleta Sandstones.

Discrimination function analysis has been used extensively to investigate the chemical composition and also to discriminate between various tectonic environments and sedimentary provenances (Fatima and Khan 2012; Ahmad et al. 2014). Using major oxide ratios as variables, discriminant function diagrams have been proposed by Roser and Korsch (1988) to distinguish sediments derived from mafic, intermediate, felsic igneous, and quartzose sedimentary rock provenance. These function further discriminate among four tectono-magmatic provenance, P1—demonstrated as Oceanic island arc, P2—mature island arc, P3—active continental margin, and P4—mature polycyclic continental sedimentary rocks, indicating thereby that they are derived from a recycled orogenic terrain, which is considered to host granite, gneissic or quartzose sedimentary rocks (Fig. 12). The sedimentary rock samples from the present study are not restricted to one field but plot in the P4 and P1 fields, indicating that they are derived from more than one source, the sandstone is from predominantly felsic rocks and shales from mafic rocks.

The geochemistry of sedimentary rocks has been widely used to discriminate the tectonic setting of the sedimentary basin (Bhatia 1983, 1985; McLennan and Taylor 1991; Graver and Scott 1995). Major element variations are considered to reflect distinct provenance types and tectonic setting for sedimentary sequences. Bhatia (1983) and Bhatia and Crook (1986) categorized sedimentary basins into four namely oceanic island arc, continental island arc, active continental margin and passive continental margin. In the  $\text{K}_2\text{O}/\text{Na}_2\text{O}$  versus  $\text{SiO}_2$  diagram (Fig. 13) (Roser and Korsch 1986), all the studied samples occupy fields of passive margin. In  $(\text{SiO}_2/20, \text{K}_2\text{O} + \text{Na}_2\text{O}$  and  $\text{TiO}_2 + \text{Fe}_2\text{O}_3 + \text{MgO}$ ) the plot of Kroonenberg (1994), all the studied samples fall in passive margin setting (Fig. 14).

Maynard et al. (1982) provided a tectonic setting discrimination diagram based on the cross plots of  $\text{SiO}_2/\text{Al}_2\text{O}_3$  versus  $\text{K}_2\text{O}/\text{Na}_2\text{O}$ , which is used for the interpretation of tectonic setting of sedimentary basins. The plot distinguishes the passive margin basins (PM) from the active continental margin (ACM) and the arc settings, including basaltic and andesitic detritus, (A1) and the evolved arc setting (A2) (Fig. 15) All the samples of the Athleta Sandstone and Ridge Sandstone are plotted within the passive margin field, while the Ridge Shale is plotted within the active continental margin field.

## 10 Conclusions

The sandstones are generally medium to coarse grained, poorly to well sorted, and with sub-angular to sub-rounded grains, which indicates that the currents were fluctuating in condition to produce poorly to well sorted sediments. The studied rocks of Chari Formation are quartzarenite, arkose, subarkose, sublitharenite, and lithicarenite. The sediments are modified by paleoclimate, distance of transport, and diagenesis. A good to strong correlation between  $Al_2O_3$  and the other oxides in these sediments indicates clay mineral control. Based on the major element geochemical classification diagrams of Pettijohn et al. (1987) and Herron (1988), the studied samples are classified as arkose, subarkose, sublitharenite, and quartzarenite type. Various chemical-weathering indices such as the CIA, CIW, PIA and ICV suggests that Jara Dome sediments show moderate to high chemical weathering. Heavy rainfall, vegetation cover, relief, high surface temperature, and high atmosphere  $CO_2$  are the major factors which control the intensity of weathering. The scattering shown by data points in the A-CN-K diagram probably represents a variable degree of weathering in the source terrain. This may be result of no-steady state weathering conditions where active tectonism and uplift allow erosion of all soil horizons and rock surfaces (Nesbitt et al. 1997). The discriminant function diagram of Roser and Korsch (1988) indicates that the sediments are derived from more than one source. Various plots discussed above suggest a passive margin setting for the Jara Dome sediments.

**Acknowledgments** The authors gratefully thank the Chairman, Department of Geology, Aligarh Muslim University, Aligarh for providing the necessary research facilities.

## References

- Ahmad AHM, Khan AF, Saikia C (2008) Palaeoenvironment and diagenesis of Middle Jurassic Athleta Sandstones, Jhurio Dome, Kachchh, Gujarat. *J Geol Soc India* 71:73–78
- Ahmad AHM, Noufal KN, Masroor AM, Khan T (2014) Petrography and geochemistry of Jumara Dome sediments, Kachchh Basin: implications for provenance, tectonic setting and weathering intensity. *Chin J Geochem* 33(1):9–23
- Ahmad AHM, Agarwal R, Irshad R (2015) Petrographical and geochemical studies of Proterozoic sandstones of Patherwa Formation, Son Valley, India: implication for provenance and weathering history. *Arab J Geosci* 8:1977–1991
- Balagopal AT, Srivastava VK (1975) A study of the paleocurrent and the provenances of the Jurassic rocks of Central Kutch, Gujarat state. *Indian J Earth Sci* 2:62–76
- Bardan S, Datta K (1987) Biostratigraphy of Jurassic Chari Formation: a study in Keera dome, Kutch, Gujarat. *J Geol Soc India* 30:121–131
- Bhatia MR (1983) Plate tectonics and geochemical composition of sandstones. *J Geol* 91:611–627
- Bhatia MR (1985) Rare earth element geochemistry of Australian Paleozoic greywacke and mud rocks: provenance and tectonic control. *Sed Geol* 45:77–113
- Bhatia MR, Crook KAW (1986) Trace elements characteristics of greywacke and tectonic setting discrimination of sedimentary basins. *Contrib Mineral Petrol* 92:181–193
- Biswas SK (1977) Mesozoic rock stratigraphy of Kutch, Gujarat. *Quart J Geol Min Met Soc India* 49:1–52
- Biswas SK (1982) Rift basins in western margin of India and their hydrocarbon prospects with special reference of Kutch Basin. *Bull Am Assoc Pet Geol* 65:1497–1515
- Biswas SK (1987) Regional tectonic framework, structure and evolution of the western marginal basins of India. *Tectonophysics* 135:307–327
- Cannon RJ, Siambi WMNS, Karanja FM (1981) The Proto-Indian Ocean and probably Paleozoic/Mesozoic tri-radial rift system in East Africa. *Earth Planet Sci Lett* 52:419–426
- Cashyap SM, Aslam M (1992) Deltaic and shoreline sedimentation in Saurashtra basin, Western Indian: an example of infilling in an early Cretaceous failed rift. *J Sedim Petrol* 62:972–991
- Chandler MA, Rind D, Ruedy R (1992) Pangean climate during early Jurassic GCMS simulations and sedimentary record of Paleoclimate. *Geol Soc Am Bull* 104:543–559
- Chatterjee S, Hotton N III (1986) The paleoposition of India. *J Southeast Asia Earth Sci* 1:145–189
- Cox R, Lowe DR, Cullers RD (1995) The influence of sediment recycling and Basement composition on evolution of mudrock chemistry in the southwestern United States. *Geochim Cosmochim Acta* 59:2919–2940
- Dickinson WR (1985) Interpreting relations from detrital modes of sandstone. In: Zuffa GG (ed) *Provenance of arenites*. Reidel, Dordrecht-Boston-Lancaster, pp 333–361
- Dubey N, Chatterjee BK (1997) Sandstones of Mesozoic Kachchh Basins: their provenance and basinal evolution. *Indian J Pet Geol* 6:55–58
- Fatima S, Khan MS (2012) Petrographic and geochemical characteristics of Mesoproterozoic Kumbalgarh clastic rocks, NW Indian shield: implications for provenance, tectonic setting, and crustal evolution. *Int Geol Rev* 54(10):1113–1144
- Fedo CM, Nesbitt HW, Young GM (1995) Unraveling the effects of potassium metasomatism in sedimentary rocks and paleosols, with implications for weathering conditions and provenance. *Geology* 23:921–924
- Folk RL (1980) *Petrology of sedimentary rocks*. Hemphills, Austen
- Franzinelli E, Potter PE (1983) Petrology, chemistry and texture of modern river sands, Amazon River system. *J Geol* 91:23–39
- Friedman GM, Johnson KG (1982) *Exercises in sedimentology*. Wiley, New York, pp 65–99
- Fürsich FT, Pandey DK, Callomon JH, Jaitely AK, Singh IB (2001) Marker beds in Jurassic of Kachchh Basin, western India: their depositional environment and sequence-stratigraphic significance. *J Paleontol Soc India* 46:173–198
- Graver JI, Scott TJ (1995) Trace elements in shale as indicators of crustal provenance and terrain accretion in south Canadian cordillera. *Geol Soc Am Bull* 107:440–453
- Herron MM (1988) Geochemical classification of terrigenous sands and shales from core or log data. *J Sedim Petrol* 58:820–829
- Khan AF (2010) *Sedimentology of Middle Jurassic to Upper Jurassic rocks of Jhurio Dome, Kachchh, Gujarat*. Unpublished Ph.D. Thesis, Aligarh Muslim University, Aligarh
- Koshal VN (1984) Differentiation of Rhaetic sediments in the subsurface of Kutch based on palynofossils. *Pet Asia J* 7:102–105
- Kroonenberg SB (1994) Effect of provenance, sorting and weathering on the geochemistry of fluvial sand from different tectonic and climate environments. In: *Proceedings of the 29th international geological congress, Part A*, pp. 69–81

- Krynine PD (1946) Microscopic morphology of quartz types. An. 2nd Cong. Panames. Ing Minas Geol 3:35–49
- Krynine PD (1948) The megascopic study and field classification of sedimentary rocks. *J Geol* 56:130–165
- Maynard JB, Valloni R, Yu H (1982) Composition of modern deep sea sands from arc-island basin. *Geol Soc Lond Spec Publ* 10:551–561
- McLennan SM, Taylor SR (1991) Sedimentary rocks and crustal evolution, tectonic setting and secular trends. *J Geol* 99:1–21
- Nesbitt HW, Young GM (1982) Early proterozoic climates and plate motion inferred from major element chemistry of lutites. *Nature* 299:715–717
- Nesbitt HW, Fedo CM, Young GM (1997) Quartz and feldspar stability, steady and non-steady-state weathering and pedogenesis of siliciclastics sands and muds. *J Geol* 105:173–191
- Pettijohn FJ (1975) *Sedimentary rocks*. Harper and Brothers, New York, p 628
- Pettijohn FJ, Potter PE, Siever R (1987) *Sand and sandstone*. Springer, New York
- Rajnath (1932) A contribution to the stratigraphy of Kutch. *Geol Miner Soc India* 4:161–174
- Roser BP, Korsch RJ (1986) Determination of tectonic setting of sandstone–mudstone suites using SiO<sub>2</sub> content and K<sub>2</sub>O/Na<sub>2</sub>O ratio. *J Geol* 94:635–650
- Roser BP, Korsch RJ (1988) Provenance signatures of sandstone–mudstone suites determined using discrimination function analysis of major-element data. *Chem Geol* 67:119–139
- Singh CSP, Jaitley AK, Pandey DK (1982) First report of some Bajocian Bathonian (Middle Jurassic) ammonoides and the age of the oldest sediments from Kachchh. Newsletters on stratigraphy, Western India. *J Geol Soc India* 34:152–160
- Suttner LJ, Dutta PK (1986) Alluvial sandstones composition and paleoclimate, I, framework mineralogy. *J Sediment Petrol* 56:329–345
- Tankard AJ, Jackson MPA, Eriksson KA, Hobday DK, Hunter, Minter WEL (1982) *Crustal evolution of southern Africa: 3.8 billion years of Earth history*. Springer-Verlag, New York
- Thompson SL, Barron EJ (1981) Comparison of Cretaceous and present earth albedos: implication for the causes of Paleoclimates. *J Geol* 89:143–167
- Van der Plas L, Tobi AC (1965) A chart for judging the reliability of point counting results. *Am J Sci* 263(1):87–90
- Weltje GJ, Meijer XD, Doer PL (1998) Stratigraphic inversion of siliciclastic basin fills: a note on the distinction between supply signals resulting from tectonic and climate forcing [J]. *Basin Res* 10:129–153
- Zaigham NA, Mallick KA (2000) Bela ophiolite zone of southern Pakistan: tectonic setting and associated mineral deposit. *Geol Soc Am Bull* 112:478–489